



Development, characterization and *in vitro* evaluation of biodegradable rhein-loaded microparticles for treatment of osteoarthritis



Carolina Gómez-Gaete^{a,*}, Macarena Retamal^b, Catalina Chávez^a, Paulina Bustos^b, Ricardo Godoy^a, Pablo Torres-Vergara^a

^a Department of Pharmacy, Faculty of Pharmacy, University of Concepción, Concepción, Chile

^b Department of Clinical Biochemistry and Immunology, Faculty of Pharmacy, University of Concepción, Concepción, Chile

ARTICLE INFO

Article history:

Received 14 July 2016

Received in revised form 29 September 2016

Accepted 4 October 2016

Available online 6 October 2016

Chemical compounds studied in this article:

Rhein (PubChem CID: 10168)

Keywords:

Osteoarthritis

Rhein

Microparticles

Cytotoxic assays

Anti-inflammatory

Controlled release

ABSTRACT

Rhein is an active metabolite of the drug diacerein, whose anti-inflammatory properties have been demonstrated in both *in vitro* and *in vivo* models. However, the low oral bioavailability of rhein has limited its utility as a potential treatment of osteoarthritis (OA), a chronic inflammatory disease. In order to overcome this limitation, the aim of this work was the development of a drug delivery system intended for intra-articular administration of rhein, based on polymeric biodegradable PLGA microparticles (MPs) loaded with the drug. The MPs, prepared by the emulsion–solvent evaporation technique were characterized in terms of several parameters including morphology, encapsulation efficiency, molecular interactions between components of the formulation and *in vitro* release profiling. Furthermore, cell-based *in vitro* studies were performed to evaluate the cytotoxicity of the formulations and their effect on the release of inflammatory markers including pro-inflammatory cytokines and reactive oxygen species (ROS). Scanning electron microscopy demonstrated that the prepared MPs exhibited an almost spherical shape with smooth surface. The size distribution of the prepared MPs ranged between 1.9 and 7.9 μm , with mean diameter of $4.23 \pm 0.87 \mu\text{m}$. The optimal encapsulation efficiency of rhein was $63.8 \pm 3.0\%$. The results of powder X-ray diffraction and differential scanning calorimetry studies demonstrated that the active ingredient is partially the crystalline state, dispersed in the polymer matrix. This outcome is somewhat reflected in the release kinetics of rhein from the MPs.

The cytotoxicity evaluation, carried out in macrophages derived from THP-1 cells, showed that both rhein-loaded MPs and unloaded MPs did not significantly affect the cell viability at MP concentrations up to 13.8 μM . In lipopolysaccharide-activated macrophages, the rhein-loaded MPs significantly decreased the production of interleukin-1 β (IL-1 β) and (ROS), when compared to the unloaded MPs.

In conclusion, the results of this preliminary study suggest that an MP-based formulation of rhein could be tested in animal models of inflammation, aiming for an injectable commercial product capable of providing a therapeutic solution to patients suffering from chronic joint diseases.

© 2016 Elsevier B.V. All rights reserved.

1. Introduction

Osteoarthritis (OA) is a degenerative joint disease, characterized by destruction of the cartilage, bone damage and inflammation of synovial tissue (Alcaraz et al., 2010; Driban et al., 2010; Lorenz and Richter, 2006). The pro-inflammatory cytokine IL-1 β is thought to play a critical role in the development and progression of OA (Ashford and Williard, 2014), since it degrades the cartilage matrix, leading to the destruction of the articular cartilage. Studies have reported that the concentrations of IL-1 β in knee joint synovial fluid (SF) obtained from OA patients are higher than that observed in healthy people (Sauerschnig et al., 2014; Yang et al., 2015). Other important cytokines involved in OA include

tumor necrosis factor (TNF- α) (Kapoor et al., 2011; Roy et al., 2015; Wojdasiewicz et al., 2014).

Pharmacological treatment of OA is mainly focused on pain relief and improvement of joint function. Use of non-steroidal anti-inflammatory drugs (NSAIDs), has historically provided an appropriate control of symptoms, but their use in chronic treatments is limited by their side effects profile (Fernandes et al., 2013; Hochberg et al., 2012; Zhang et al., 2010).

Further advances in the understanding of the factors that govern the metabolic activity of cartilage and subchondral bone led to the search for chondroprotective substances capable of providing symptomatic relief with less secondary effects. These compounds, classified as symptomatic slow-acting drugs for OA (SYSADOAs), include cartilaginous matrix precursors (glucosamine, chondroitin sulfate and hyaluronic acid) (Salazar et al., 2014; Toegel et al., 2008) and cytokine modulators (diacerein) (Qvist et al., 2008).

* Corresponding author at: Universidad de Concepción, Facultad de Farmacia, Barrio Universitario S/N, Concepción, Chile.

E-mail address: cargomez@udec.cl (C. Gómez-Gaete).

Of the above-mentioned compounds, the anthraquinone derivative diacerein has received increased attention over the years because of its inhibitory effect on the actions elicited by the pro-inflammatory cytokine interleukin-1 β . As several reports supported the effects of diacerein on cartilage-based cell models, animal models and clinical trials (Mahajan et al., 2006; Bartels et al., 2010; Boileau et al., 2008; Felisaz et al., 1999; Malaguti et al., 2008; Martel-Pelletier et al., 1998; Permuy et al., 2015; Yaron et al., 1999), this drug was approved for human use, with a dose scheme of 50 mg twice daily, after meals. However, the low aqueous solubility of diacerein, relatively low oral bioavailability (Nicolas et al., 1998) and side effects including diarrhea and hepatotoxicity hampered its applicability as a first choice treatment (Fidelix et al., 2014; Louthrenoo et al., 2007; Verbruggen, 2006).

Diacerein is metabolized by acetyl esterases, generating active metabolites with anti-inflammatory and chondroprotective activities. One of these metabolites is rheim, whose actions have been extensively studied. Previous reports have shown that rheim inhibits the production of ROS, down-regulates the expression of matrix metalloproteinases and up-regulates the production of tissue inhibitor of metalloproteinase-1 in rabbit articular chondrocytes (Tamura et al., 2001). Further studies carried out in synovium and cartilage isolated from OA patients demonstrated that treatment with rheim significantly reduced the synthesis of IL-1 β and subsequent production of nitric oxide (NO), mediators responsible for the degeneration of the cartilage (Legendre et al., 2007; Martel-Pelletier et al., 1998; Moldovan et al., 2000). However, the pharmacokinetics of rheim after oral administration is very similar to the observed with diacerein, being the poor aqueous solubility responsible of the low bioavailability exhibited by the compound (Li et al., 2013; Nicolas et al., 1998; Sun et al., 2012).

Therefore, considering the therapeutic possibilities offered by rheim, its low aqueous solubility could be an advantage for the development of other drug delivery systems (Stevenson et al., 2012). In this regard, the use of polymeric microparticles (MPs) is a feasible alternative since they are capable of encapsulating drugs with low aqueous solubility, while acting as controlled release systems (Butoescu et al., 2009b). This approach aims to reduce the number of doses required to achieve the desired therapeutic effect and allow direct administration to the target tissue, hence increasing the drug concentration in the affected zone and reducing undesired side effects (Butoescu et al., 2009b). Since MPs can be formulated with biocompatible and biodegradable polymers, these properties will ensure that the formulation is completely removed from the site of action and the body after delivering the drug. Among the most widely employed polymers for development of biodegradable MPs, the poly-lactic co-glycolid acid PLGA, a co-polymer approved by the FDA, is known for its ability to degrade in the presence of water (Shive and Anderson, 1997).

Several studies have been focused on the development of a delivery system based on PLGA microparticles and other polymers for the treatment of joint diseases such as OA. These formulations are capable of encapsulating diverse types of drugs including NSAIDs (Elron-Gross et al., 2009; Fernandez-Carballido et al., 2004), corticoids (Bodick et al., 2013; Butoescu et al., 2009a) and other molecules (Gaignaux et al., 2012) with encouraging results.

In this study, the development and characterization of an intra-articular delivery system based on polymeric PLGA MPs loaded with rheim is presented. Prior to its testing in animal models, the performance of this formulation was assessed in terms of cytotoxicity and anti-inflammatory effect after stimulation with LPS in a cell-based *in vitro* model.

2. Materials and methods

2.1. Materials

Poly(lactic-co-glycolic acid) (PLGA) RESOMER® RG756s, RESOMER® RG753s, RESOMER® RG752s, were all provided by Evonik Industries (Germany). Rheim, lipopolysaccharide from *Escherichia coli* O127:B8,

phorbol 12-myristate 13-acetate (PMA), piperazine-*N'*-(2-ethanesulfonic acid) (HEPES) and poly (vinyl alcohol) (PVA, 86%–89% hydrolyzed) were purchased from Sigma-Aldrich (MO, USA). Monocyte cell line was obtained from the American Type Culture Collection (ATCC) (Manassas, VA). Methanol, 2-propanol and acetonitrile in high-performance liquid chromatography (HPLC) grade were purchased from Merck (Darmstadt, Germany).

2.2. Microparticle preparation

PLGA MPs loaded with rheim were prepared through the solvent emulsion–evaporation method. Briefly, rheim was dissolved in 2.5 mL of methanol. The resulting solution was mixed with 200 mg of PLGA dissolved in 2.5 mL of dichloromethane. The organic solution was then pre-emulsified with 20 mL of acidified 0.25% w/v PVA aqueous solution by shaking it for 1 min at 3200 rpm in a Vortex Genie 2 (Scientific Industries Inc. USA). In order to obtain a microemulsion, the pre-emulsion was homogenized for 30 s at 8000 rpm with a homogenizer system (Heidolph, Germany). The organic phase was evaporated at room temperature under gentle agitation (700 rpm) and the MPs suspension was then completed to 20 g by weight with nanopure water.

The development and optimization of the microparticulate system considered the study of parameters including the type of polymer used and the initial amount of rheim.

2.3. Physicochemical characterization of MPs

2.3.1. Extraction of rheim from microparticles

A 2 mL aliquot of MPs suspension was centrifuged in order to obtain a pellet that was washed with 1 mL methanol before breaking the MPs with 1 mL of acetone. Then, 2 mL of methanol were added to dissolve the encapsulated rheim and 1 mL of the above solution was evaporated at 40 °C with nitrogen flow. The sample was reconstituted with methanol and the solution obtained was filtered through a 0.22 μ m polyvinylidene difluoride membrane before its analysis by HPLC.

2.3.2. Quantification of rheim in samples

The amount of rheim within the MPs and its concentration in liquid samples (medium for *in vitro* release) was determined by HPLC using a validated method for each matrix. Analyses were performed in a LaChrom Elite system (Merck-Hitachi, Japan), using a Kromasil Reverse Phase C-18 column (5 μ m, 250 mm), a mobile phase composed of methanol:acetic acid solution 2% (80:20 v/v) at isocratic flow rate of 1 mL min⁻¹. The UV detection of rheim was set up at 257 nm. All the analyses were performed at room temperature (\pm 20 °C). The developed method showed satisfactory linearity between 10 and 90 μ g/mL.

The drug loading and encapsulation efficiency of the rheim-loaded MPs were calculated according to Eqs. (1) and (2):

$$\text{Drug loading (\%)} = \frac{\text{amount of rheim in MPs}}{\text{amount of microparticles}} * 100 \quad (1)$$

$$\text{Encapsulation efficiency (\%)} = \frac{\text{total amount of rheim in MPs}}{\text{theoretical amount of rheim added initially}} * 100 \quad (2)$$

2.3.3. Particle size and zeta potential

The particle size of the prepared formulations was determined by light scattering with a Mastersizer 3000 (Malvern Instruments, Worcestershire, UK), equipped with the Hydro 2000S dispersion unit. The volume mean diameter was used as a representative diameter.

The zeta potential was measured using a Nano ZS Zetasizer (Malvern Instruments, Worcestershire, UK) based on quasi-elastic light scattering at 25 °C following 1/100 (v/v) dilution in purified water. The values reported represent the average of three measurements.

2.3.4. Scanning electron microscopy

Scanning electron microscopy of the formulations was performed with a JSM 6380 LV system (JEOL Techniques Ltd., Tokyo, Japan), operating at a 20 kV accelerating voltage. The MPs were coated with a gold layer of about 150 Å in thickness, using an Edwards S 150 sputter coater (Agar Scientific, Standsted, UK).

2.3.5. X-ray diffraction (XRD)

XRD patterns were measured on an X-ray diffractometer, D4 EN-DEAVOR (Bruker AXS, USA) using Ni-filtered Cu K α_1 radiation and operated at 40 kV and 20 mA. The step width was 0.02° with 5 s counting time per step; the samples were run between 3° and 60° 2 θ .

2.3.6. Differential scanning calorimetry (DSC)

DSC curves for the raw materials, physical mixture, empty MPs and rhein-loaded MPs were obtained from a DSC-822e system (Mettler Toledo, Columbus, OH, USA) equipped with a EK90/MT intra-cooler (Haake, Germany). Samples were heated in sealed standard aluminum pans from 0 °C to 400 °C under a dynamic nitrogen atmosphere at a scanning rate of 10 °C/min, with an empty aluminum pan as reference.

2.3.7. In vitro release kinetics of rhein from microparticles

In vitro release studies were performed through the dialysis bag diffusion technique, using 10 mM HEPES saline buffer (150 mM NaCl, pH 7.4) as medium. An amount of MPs, equivalent to 5 mg of rhein, was resuspended in 5 mL of HEPES saline buffer by vortexing and placed into a dialysis membrane previously soaked overnight in water (molecular weight cutoff (MWCO): 12,000 Da, Sigma Chem., USA). The dialysis membrane containing the dispersed MPs was placed into a 250-mL beaker filled with 245 mL of HEPES saline buffer and the experiment was performed at 37 °C on a Venticell oven (MMM Medcenter Einrichtungen, Germany) with stirring rate of 300 rpm (Multistirrer 6, Velp® Scientifica). At fixed time intervals, the samples were withdrawn from the outer aqueous solution and replaced with fresh same release medium to maintain constant volume and sink condition. The released rhein was quantified by HPLC. Every experiment was performed in triplicate.

2.4. Cell assays

2.4.1. Cell line and culture condition

The THP-1 human acute monocytic leukemia cell line (ATCC, American Type Culture Collection) was cultured in RPMI-1640 medium supplemented with 10% heat-inactivated fetal bovine serum, 1 mM sodium pyruvate, 10 mM of HEPES, 140 mM of glucose, 0.05 mM 2-mercaptoethanol and penicillin/streptomycin in an atmosphere of 5% CO₂ and 37 °C. For the induction of monocyte–macrophage differentiation, THP-1 cells were seeded in 96-well plates at a cell density of 1×10^6 cells/mL in RPMI 1640 medium with 100 ng/mL of PMA and incubated for 24 h. After differentiation, the non-attached cells were removed by aspiration and the adherent macrophages were washed with RPMI 1640 medium.

2.4.2. Cell viability assay

Prior to the *in vitro* cell-based experiments, both empty and rhein-loaded MPs were sterilized by gamma irradiation at 2.5 Mrad. Further experiments demonstrated that neither the loading of rhein nor the release kinetics were affected by the sterilization procedure (data not shown).

Cytotoxicity of empty and rhein-loaded MPs on differentiated cells was measured by means of MTT assay, using the Vybrant® MTT cell proliferation assay Kit (Invitrogen, Carlsbad, CA, USA). THP-1 macrophages stimulated with 5 ng/mL LPS were treated for 24 h and 48 h with either control medium or medium supplemented with increasing concentrations of MPs. After treatment, the MTT solution (12 mM) was added and incubated for 3 h. Finally, the MTT solution was removed and

incubated for another 12 h with 100 μ L of SDS-HCl solution to solubilize the formed formazan crystals. Optical density was measured at 570 nm with a microplate reader (Synergy 2, BioTek Instruments, USA). Viability of cells was quantified as a percentage compared to the control (Eq. (3)):

$$\text{Cell viability (\%)} = \frac{\text{absorbance in sample}}{\text{absorbance in control}} * 100 \quad (3)$$

2.4.3. Enzyme-linked immunosorbent assay for quantification of interleukin-1 β (IL-1 β) and tumor necrosis factor alpha (TNF- α)

LPS-stimulated THP-1 macrophages were incubated with different concentrations of both empty and rhein-loaded sterilized MPs at a concentration range equivalent to 0–27.5 μ M for 24 h. After LPS stimulation and further treatment with MPs, the cell-free supernatants were collected and used for measurement of cytokine concentrations with ELISA kits for IL-1 and TNF- α , according to the manufacturer's instructions (Ready-SET-Go!®, eBioscience Inc., San Diego, CA, USA). The optical density from the individual wells was measured using a microplate reader at 450 nm (Synergy 2, BioTek Instruments, USA).

2.4.4. Measurement of intracellular reactive oxygen species (ROS)

The intracellular production of ROS by LPS-stimulated macrophages was estimated by using the fluorescent dye dichlorofluorescein diacetate (DCFH-DA). Cells were treated with both empty and rhein-loaded sterilized MPs at indicated concentrations for 24 h. After addition of 200 μ L of DCFH-DA dye (final concentration of 10 μ M), the cells were incubated at 37 °C for 30 min. The fluorescence intensity was determined at λ_{ex} 485 nm and λ_{em} 540 nm. Differentiated THP-1 cells treated with hydrogen peroxide (500 μ M) were used as a positive control.

2.5. Statistical analysis

Statistical analysis was performed by means of a 2-way analysis of variance (ANOVA) test, using the Prism 6 software (GraphPad, USA).

3. Results and discussion

3.1. Effect of the polymer employed and initial drug amount on loading and encapsulation efficiency

In order to ensure an appropriate loading of rhein within the prepared MPs, the effect of the polymer employed on the encapsulation efficiency of the drug was investigated. This study was carried out using three polymers described in the methodology and Table 1; the MPs were prepared by maintaining constant certain formulation parameters including the amount of polymer and rhein. Results are shown in Table 1.

From the encapsulation efficiency and loading % values presented in Table 1, an inverse relationship between both parameters and the viscosity of the polymer can be observed. This outcome could be explained by the fact that when rhein is added to the polymer solution, a suspension is formed, and the polymers with higher viscosities might prevent the homogenous dispersion of the drug, forming agglomerates that may negatively affect the encapsulation process. Therefore, the RG 752s polymer was chosen for subsequent studies.

Since only one fixed amount (5 mg) of rhein was employed for the above-described experiment, the effect of increasing initial amounts of rhein on the drug loading and encapsulation efficiency was studied. For each formulation batch, the above-mentioned parameters were calculated and the results are presented in Fig. 1.

From the graph, it can be noticed that the loading of rhein within the MPs is positively influenced by the initial amount of drug in the formulation, but at the expense of encapsulation efficiency. By superimposing both curves, the best result is obtained with an initial amount of 5 mg.

Table 1
Effect of polymer viscosity on rhein encapsulation efficiency and loading.

Polymer	Composition	Viscosity (dL/g)**	Encapsulation efficiency (% ± SD)*	Loading (% ± SD)*
RG752s	PLGA 75:25 with ester-end group	0.16–0.24	63.8 ± 3.0	1.60 ± 0.07
RG753s	PLGA 75:25 with ester-end group	0.32–0.44	39.4 ± 2.7	0.99 ± 0.06
RG756s	PLGA 75:25 with ester-end group	0.71–1.0	32.5 ± 3.3	0.81 ± 0.08

* Experiments with each polymer were performed in triplicate.

** Inherent viscosity (0.1% in chloroform at 25 °C).

3.2. Particle size, morphology and zeta potential

The size distribution of the prepared MPs ranged between 1.9 and 7.9 μm , with mean diameter of $4.23 \pm 0.87 \mu\text{m}$.

Since the formulated MPs are designed to enter the joint cavity, size is a parameter of great importance for the effectiveness and safety of the treatment, as it directly influences the retention of the drug in the joint and the immune response that could trigger either the inflammatory response or activation of phagocytic cells (Butoescu et al., 2009b).

Some reports claim that the administration of MPs larger than 10 μm to the joint cavity may cause swelling of the zone (Horisawa et al., 2002; Howie et al., 1993), while MPs with sizes between 1 and 4 μm can be phagocytosed by macrophages without inducing the local immune response mediated by neutrophils (Edwards, 2011). Although the phagocytosis of MPs may contribute to a faster degradation of the polymeric matrix, this phenomenon is not entirely detrimental as the MPs would continue the release process of rhein within the phagocytes and in turn directly act over them, reducing the joint damage (Champion et al., 2008). Furthermore, the loss of the MPs by normal synovial fluid purification would be reduced as they remain inside of the cells that comprise the joint (Ratcliffe et al., 1984; Ratcliffe et al., 1987).

The morphological characteristics of the prepared rhein-loaded MPs are shown in Fig. 2.

From the SEM images, it can be observed that the MPs exhibit a spherical shape, smooth surface and absence of pores. The smooth surface of the microparticles may be due to the use of PVA in the formulation, which acts as a stabilizer of the emulsion, preventing coalescence of the beads from the organic phase during the preparation process (Lee et al., 1999).

The measured zeta potential of the prepared rhein-loaded MPs was -21.4 mV . Previous reports have established that values near 30 mV are appropriate to ensure the stability of the formulations in suspension, since there is a balance between the repulsion and attraction forces of the dispersed particles in the medium, avoiding the formation of aggregates that difficult the re-dispersion of the MPs.

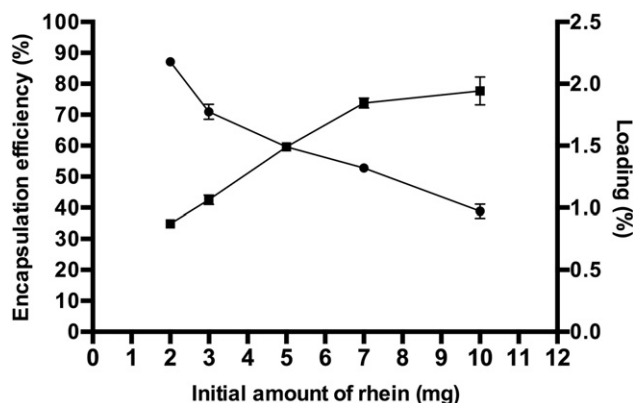


Fig. 1. Effect of the initial amount of rhein on the loading (■) and encapsulation efficiency (●) within MPs. Data represent the mean ± SD of at least three independent experiments.

3.3. Structural analysis

The interactions between the components structuring the microparticulate system and rhein were assessed by means of powder X-ray diffraction and differential scanning calorimetry analyses.

3.3.1. Powder X-ray diffraction

The results of the powder X-ray diffraction analyses for raw materials, unloaded MPs and rhein-loaded MPs are presented in Fig. 3.

The diffraction pattern of rhein shows sharp peaks at 9.9, 11, 17.7 and 27.7 two-theta scale, indicating the crystalline nature of the molecule, while the PLGA polymer and unloaded MPs patterns exhibit the characteristic behavior of compounds in the amorphous state. In the case of the rhein-loaded MPs, the diffraction pattern shows a small peak at 27.7 two-theta scale, also present in the physical mixture. This result suggests that rhein still can be found in a crystalline state, but probably dispersed in the polymer matrix.

3.3.2. Differential scanning calorimetry (DSC)

The DSC curves for raw materials, unloaded MPs and rhein-loaded MPs are shown in Fig. 4.

Analysis of the rhein DSC curve shows a single endothermic peak at 334.8 °C (range 320 °C–350 °C), attributable to the melting of the drug. This finding was confirmed through thermogravimetric analysis (data not shown). The DSC curve obtained from PLGA exhibited two endothermic peaks, being the first located at 60 °C (range 50 °C–65 °C) which corresponds to the glass transition temperature (T_g), characteristic of amorphous polymers. The second peak, found at 364 °C (range 270 °C–400 °C), is representative of polymer decomposition.

In the physical mixture curve, the endothermic peak assigned to rhein is not observed, probably due to the small amount in the sample. The glass transition peaks of PLGA are still present for both the physical mixture and empty MPs, but in the latter there is a marked reduction of the enthalpy associated to the glass transition (from 112.91 mJ to 77.76 mJ) that may be explained by the structural relaxation of the polymer elicited by the preparation process (Allison, 2008). This decrease in the enthalpy values is also observed in the rhein-loaded MPs (from 112.91 mJ to 47.53 mJ) and is accompanied by a reduction of T_g from 60.76 °C to 58.78 °C. In addition, although not seen in the presented figure, there is a small endothermic peak at 329.4 °C that may correspond to rhein in its crystalline state. The results suggest that a fraction of rhein could be present at the crystalline state and embedded within the polymeric matrix, hence modifying the T_g of PLGA.

3.4. In vitro release kinetics

The results of the *in vitro* release kinetics of rhein encapsulated on PLGA MPs are presented in Fig. 5. The diffusion from the dialysis membrane and further dissolution of non-encapsulated rhein, used as reference for this study, occurred within 24 h. The release profile of encapsulated rhein shows that approximately 45% of the total amount present in the formulation was released before 24 h, suggesting that an important fraction of the drug is adsorbed to the surface or encapsulated in the outer layers of the MP. This finding is in agreement with the results obtained in the XRD and DSC studies, which suggest that rhein

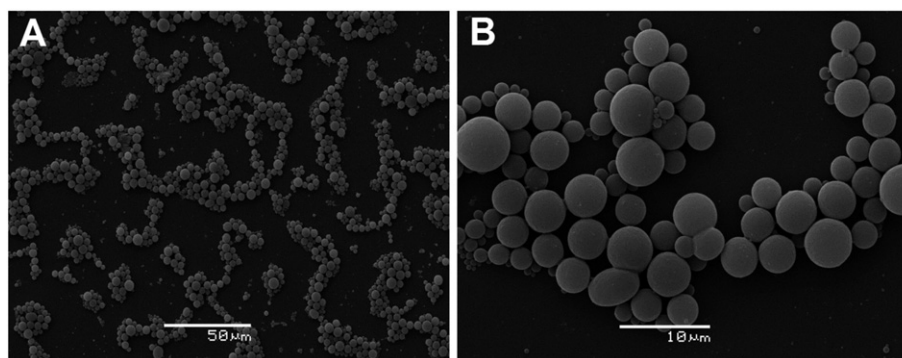


Fig. 2. Scanning electron microscopic image of rhin-loaded MPs. (A) General picture of the field. (B) A magnification of the image.

could exist at the crystalline state. After this time interval, the diffusion of rhin was slower but consistent over the testing period, reaching 90% of drug released after 30 days.

The release profile of rhin from the MPs exhibits the characteristic behavior of bioerodible polymeric drug delivery systems, which includes an initial “burst” release effect, followed by a semi-“zero order” and final rapid release phases. The above-mentioned phases occur due to physicochemical interactions between the aqueous medium and the MPs, such as (1) water imbibition into the system; (2) drug dissolution (if the drug is not molecularly dispersed throughout the system); (3) polymer chain cleavage; (4) diffusion of the drug and polymer degradation products out of the device (because of concentration gradients); (5) the creation of water-filled pores and (6) the breakdown of the polymeric structure once the system becomes unstable (Siepmann et al., 2002).

In order to analyze the morphological changes occurring in the MPs during the drug release study, the remaining formulation contained in the dialysis membrane at the end of the experiment was observed through SEM (Fig. 6A). In the micrographs, it is clearly seen that the MPs are not completely degraded, but there is a marked presence of pores in the surface (Fig. 6B). This outcome suggests that rhin may be released from the MPs by a combination of diffusion and erosion of the polymeric matrix.

3.5. Cell assays

3.5.1. MTT cell viability assay

The effect of increasing concentrations of both empty and rhin-loaded MPs, in the range of 0 to 27.5 μM , on the viability of THP-1 cells after a 24 h and 48 h treatment is presented in Fig. 7.

Analysis of the data revealed that neither the time of treatment nor the loading with rhin had a significant effect on cell viability when

compared to the control condition at concentrations up to 13.8 μM . A 24 h treatment with both empty and rhin-loaded MPs at a concentration of 27.5 μM elicited a reduction of the cell viability that became significant after 48 h of treatment. Since this formulation is intended for use in chronic patients who are subjected to long-term treatments, this outcome allowed to discard this high concentration in further experiments even although some authors suggest that materials providing cell viability values over 80% are considered to be biocompatible (Campos et al., 2013). As there is no guarantee that other cellular processes are not being affected by the exposure to the MP formulations at concentrations higher than 13.8 μM , it was decided to assay concentrations that kept cell viability values over 95%.

In the present study, the effects of rhin as single treatment were not investigated. The rationale behind this decision lied on the design of the study, which utilized empty MPs as control for each treatment tested. Furthermore, the final concentration of rhin in the MP formulations was close to the maximum levels reached in synovial fluid (10^{-5} M) (Martel-Pelletier and Pelletier, 2010) and between the range tested in human synovial fibroblasts (Yaron et al., 1999) or the above described THP-1 cells (Heo et al., 2010).

3.5.2. Effect of treatment with rhin-loaded microparticles on the production of pro-inflammatory cytokines and reactive oxygen species

The results of the effect elicited by rhin-loaded MPs on the production of IL-1 β , TNF α and ROS in LPS-stimulated macrophages, are presented in Fig. 8.

From the graph, it can be inferred that rhin-loaded MPs are capable of inhibiting, in a significant and concentration-dependent manner, the

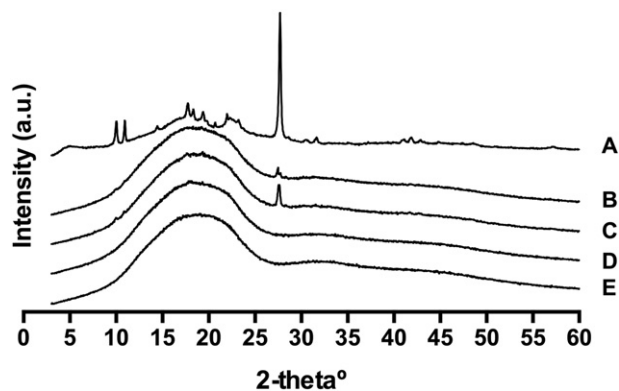


Fig. 3. X-ray diffraction patterns for the formulation components including (A) rhin, (B) rhin-loaded MPs, (C) physical mixtures of the formulation components, (D) unloaded MPs and (E) PLGA.

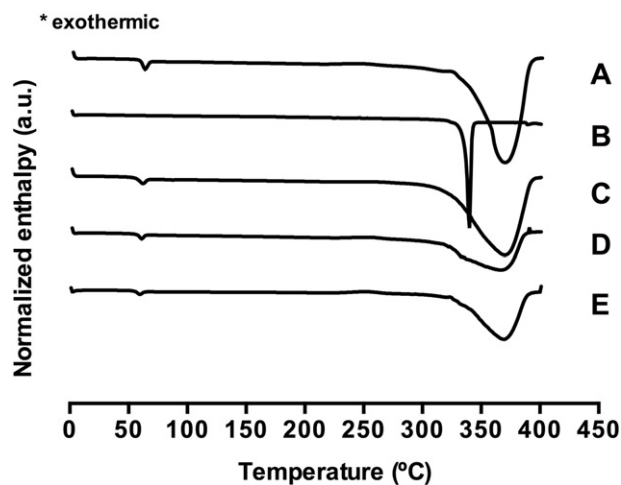


Fig. 4. Differential scanning calorimetry curves for the formulation components. (A) PLGA, (B) rhin, (C) physical mixture of the formulation components, (D) rhin-loaded MPs and (E) unloaded MPs.

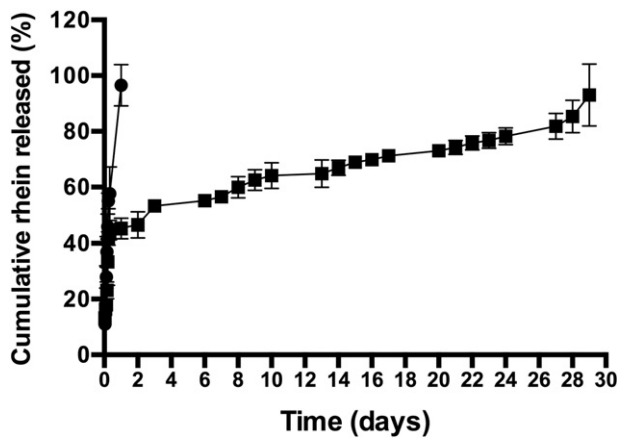


Fig. 5. Drug release profile of rhein as free drug (●) and rhein encapsulated into MPs (■). Data represent the mean \pm SD of at least three independent experiments.

production of IL-1 β and ROS when compared to the control medium and empty MPs. However, this outcome was not replicated in the case of TNF α , since the rhein-loaded formulation only exerted a significant reduction on the levels of the cytokine when compared to the control and empty MPs at the lowest tested MP concentration (1.7 μ M). Since the *in vitro* release kinetics of rhein encapsulated into MPs demonstrated that 45% is released (of the amount loaded) to the medium after 24 h of incubation, the effects observed can be safely attributed to the presence of free drug.

According to the presented findings, the inhibitory effect of the prepared rhein-loaded MPs on IL-1 β production is consistent with previous studies of free drug conducted in synoviocytes, cultured human chondrocytes and THP-1 cells (Moldovan et al., 2000; Tamura et al., 2002; Yaron et al., 1999). These reports attribute the effects of rhein on IL-1 β production as a result of the inhibition of the nuclear transcription factor- κ B (NF- κ B) pathway, decreasing the transcription of genes for various pro-inflammatory cytokines including IL-1 β and TNF α . However, other signaling pathways including the kinase c-jun N-terminal (JNK), p38 MAPK also mediate the biological effects of IL-1 β and TNF α (Sokolove and Lepus, 2013; Tak and Firestein, 2011). The induction of pro-inflammatory mediators by LPS stimulation is regulated by NF- κ B and the activator protein-1 (AP-1) at the transcriptional level, so the inhibition of one or both of them has marked effects on the mRNA levels of iNOS, IL-6, IL-1 β and TNF α (Chen et al., 2014; Gao et al., 2014b; Lee et al., 2006; Yang et al., 2012).

The lack of a marked effect elicited by the rhein-loaded MPs on the production of TNF α may be partially explained by evidence reported

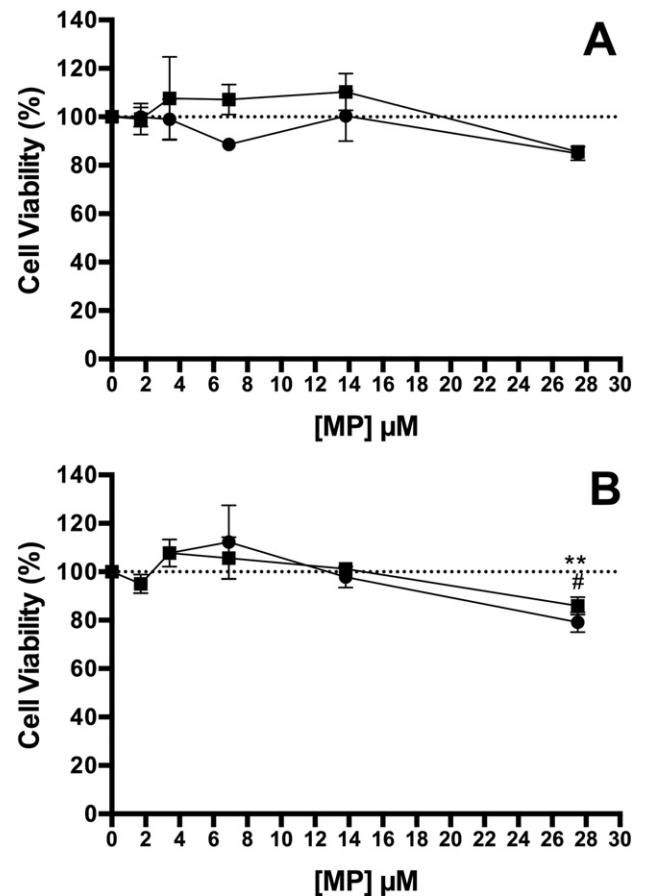


Fig. 7. Effects of MPs on cell viability. LPS stimulated macrophages were incubated with empty (●) and rhein-loaded (■) MPs for 24 h (A) and 48 h (B) and the cell viability was evaluated by MTT assay. Dashed line represents the control values. Data represent the mean \pm SD of at least three independent experiments; each experiment was performed in triplicate. **, ($p < 0.01$) control without MPs vs. empty MPs; #, ($p < 0.05$) control without MPs vs. rhein-loaded MPs.

by Gao et al., who suggest a differential effect of rhein on the LPS-mediated activation of NF- κ B and AP-1 in the RAW 264.7 immortalized cell line (Gao et al., 2014a). This report demonstrated that the inhibition of NF- κ B activity by rhein occurs through inhibition of IKK β phosphorylation, which decreased the LPS-induced mRNA expression of IL-1 β and TNF α . However, despite this inhibition at the genomic level, there was a further increase in the production of IL-1 β and TNF α , which suggests

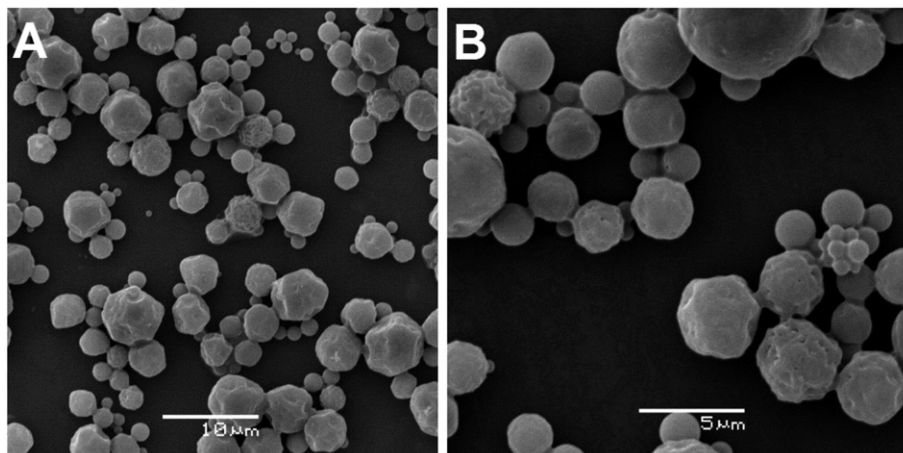


Fig. 6. Scanning electron microscopic image of typical MPs loaded with rhein after an *in vitro* release study. (A) General picture of the field. (B) A magnification of the image in which one can clearly see the surface of the particles.

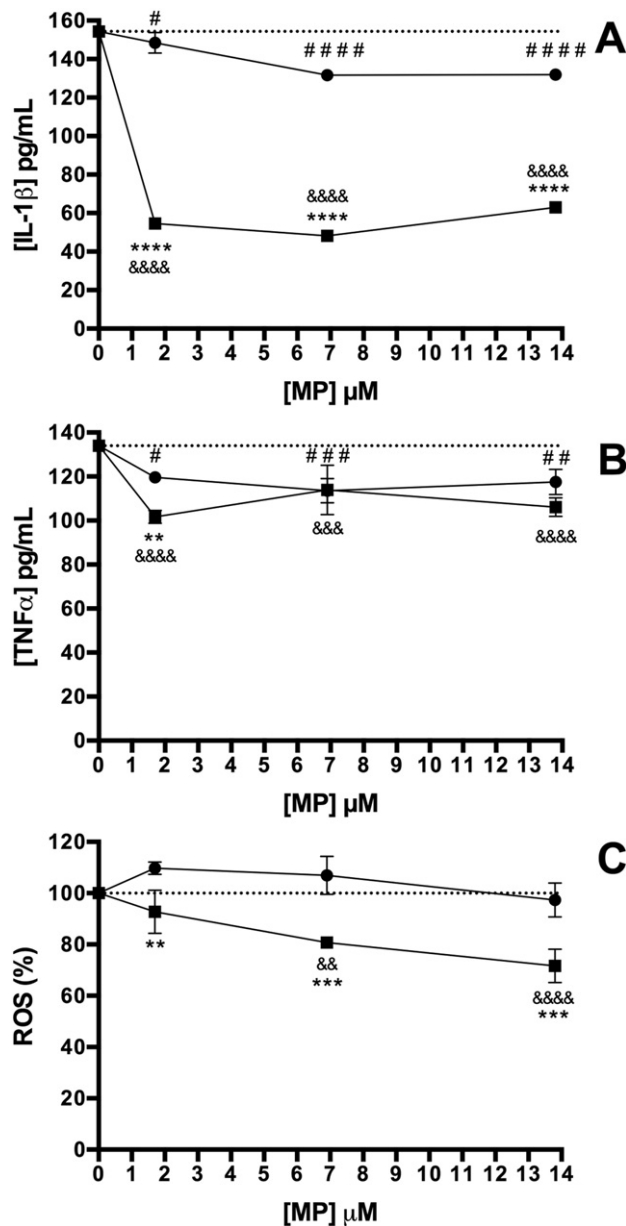


Fig. 8. Effects of empty (●) and rhein-loaded (■) MPs on the production of (A) IL-1 β , (B) TNF α and (C) ROS. Dashed line represents the control values. Data represent the mean \pm SD of at least three independent experiments; each experiment was performed in triplicate. **, ($p < 0.01$) empty MPs vs. rhein-loaded MPs; ***, ($p < 0.001$) empty MPs vs. rhein-loaded MPs; ****, ($p < 0.0001$) empty MPs vs. rhein-loaded MPs; #, ($p < 0.05$) control without MPs vs. empty MPs; ##, ($p < 0.01$) control without MPs vs. empty MPs; ###, ($p < 0.001$) control without MPs vs. empty MPs; ####, ($p < 0.0001$) control without MPs vs. empty MPs; &, ($p < 0.05$) control without MPs vs. rhein-loaded MPs; &&, ($p < 0.01$) control without MPs vs. rhein-loaded MPs; &&&, ($p < 0.001$) control without MPs vs. rhein-loaded MPs; &&&&, ($p < 0.0001$) control without MPs vs. rhein-loaded MPs.

that the LPS-induced production of pro-inflammatory cytokines may be regulated by other mediators and transcriptional factors, as demonstrated Gao et al. (2014a) and other authors (Greten et al., 2008). Since treatment with rhein did not alter the activity of AP-1 in the study of Gao et al. (2014a), this signaling pathway could compensate the rhein-mediated inhibition of NF- κ B in LPS-stimulated macrophages.

The production of reactive oxygen species (ROS) is an important part of the mechanism of generation and maintenance of the inflammatory environment in osteoarthritis. The oxidative stress induced by ROS acts as a second messenger in pro-inflammatory signaling pathways (Marinho et al., 2014) and is acknowledged that a reduction in the

production of ROS is often associated with a decrease in the inflammatory response. In this regard, the findings of the present study are validated by the previously mentioned premise. However, there is evidence that proves the contrary since the same study by Gao et al. (2014a), previously cited in this discussion, demonstrated that rhein significantly reduced the levels of ROS while increasing the release of IL-1 β on the RAW 264.7 cell line. An explanation behind this paradoxical phenomenon lies on findings that demonstrated the inhibitory effect of high intracellular superoxide anion concentrations on the activity of caspase-1, the enzyme responsible for the conversion of pro-IL-1 β to its active form, in primary mouse peritoneal macrophages (Meissner et al., 2008).

Although the findings of the present study are not in concordance with some aspects of the above-described evidence, there are certain issues worth mentioning. First, the exposure of LPS-stimulated macrophages to rhein released from the MPs is not direct like in the previously mentioned reports since the drug is being released from a polymeric matrix, so there could be concentration-dependent effects that might influence the outcome. Second, as another cell line was employed in this study, the presence of cell-specific responses calls for a cautious comparison of results. Nevertheless, this preliminary exploration of the interactions between the formulated rhein-loaded MPs and a competent *in vitro* cell model of inflammation provides consistent evidence that the developed drug delivery system has the potential to perform in animal models of osteoarthritis.

4. Conclusions

Treatment of joint diseases such as osteoarthritis still represents a challenge due to the inherent complications of administering long-term treatments with drugs known to cause severe local and systemic adverse effects. The development of controlled release formulations represents a feasible alternative for future therapies and in this regard, the results obtained in this preliminary work show promise. The developed MPs loaded with rhein were capable of providing a sustained release of the drug over a month and reduced the release of pro-inflammatory mediators in an *in vitro* cell-based model of inflammation. This outcome set the trend for further work, which will be focused on studying the effects of this formulation on animal *in vivo* models of osteoarthritis.

5. Declaration of interest

The authors report no declarations of interest.

Acknowledgments

The authors would like to thank the Chilean Council for Science and Technology, CONICYT, FONDECYT Project No. 1140706, Project ENLACE No. 213.074.050-1.0 and CD UCO 1201 of University of Concepcion.

References

- Alcaraz, M.J., Megias, J., Garcia-Arnandis, I., Clerigues, V., Guillen, M.I., 2010. New molecular targets for the treatment of osteoarthritis. *Biochem. Pharmacol.* 80, 13–21.
- Allison, S.D., 2008. Effect of structural relaxation on the preparation and drug release behavior of poly(lactide-co-glycolic)acid microparticle drug delivery systems. *J. Pharm. Sci.* 97, 2022–2035.
- Ashford, S., Williard, J., 2014. Osteoarthritis: a review. *Nurse Pract.* 39, 1–8.
- Bartels, E.M., Bliddal, H., Schöndorff, P.K., Altman, R.D., Zhang, W., Christensen, R., 2010. Symptomatic efficacy and safety of diacerein in the treatment of osteoarthritis: a meta-analysis of randomized placebo-controlled trials. *Osteoarthr. Cartil.* 18, 289–296.
- Bodick, N., Lufkin, J., Willwerth, C., Blanks, R.C., Inderjeeth, C.A., Kumar, A., Clayman, M.D., 2013. Fx006 prolongs the residency of triamcinolone acetone in the synovial tissues of patients with knee osteoarthritis. *Osteoarthr. Cartil.* 21, S144–S145.
- Boileau, C., Tat, S.K., Pelletier, J.P., Cheng, S., Martel-Pelletier, J., 2008. Diacerein inhibits the synthesis of resorptive enzymes and reduces osteoclastic differentiation/survival in osteoarthritic subchondral bone: a possible mechanism for a protective effect against subchondral bone remodelling. *Arthr. Res. Ther.* 10, R71.

- Butoescu, N., Jordan, O., Burdet, P., Stadelmann, P., Petri-Fink, A., Hofmann, H., Doelker, E., 2009a. Dexamethasone-containing biodegradable superparamagnetic microparticles for intra-articular administration: physicochemical and magnetic properties, in vitro and in vivo drug release. *Eur. J. Pharm. Biopharm.* 72, 529–538.
- Butoescu, N., Jordan, O., Doelker, E., 2009b. Intra-articular drug delivery systems for the treatment of rheumatic diseases: a review of the factors influencing their performance. *Eur. J. Pharm. Biopharm.* V 73, 205–218.
- Campos, E., Branquinho, J., Carreira, A.S., Carvalho, A., Coimbra, P., Ferreira, P., Gil, M.H., 2013. Designing polymeric microparticles for biomedical and industrial applications. *Eur. Polym. J.* 49, 2005–2021.
- Champion, J.A., Walker, A., Mitragotri, S., 2008. Role of particle size in phagocytosis of polymeric microspheres. *Pharm. Res.* 25, 1815–1821.
- Chen, X., Zong, C., Gao, Y., Cai, R., Fang, L., Lu, J., Liu, F., Qi, Y., 2014. Curcumin exhibits anti-inflammatory properties by interfering with the JNK-mediated AP-1 pathway in lipopolysaccharide-activated RAW264.7 cells. *Eur. J. Pharmacol.* 723, 339–345.
- Driban, J.B., Sittler, M.R., Barbe, M.F., Balasubramanian, E., 2010. Is osteoarthritis a heterogeneous disease that can be stratified into subsets? *Clin. Rheumatol.* 29, 123–131.
- Edwards, S.H., 2011. Intra-articular drug delivery: the challenge to extend drug residence time within the joint. *Vet. J.* 190, 15–21 (London, England : 1997).
- Elron-Gross, I., Glucksam, Y., Biton, I.E., Margalit, R., 2009. A novel Diclofenac-carrier for local treatment of osteoarthritis applying live-animal MRI. *J. Control. Release* 135, 65–70.
- Felisz, N., Boumediene, K., Ghayor, C., Herrouin, J.F., Bogdanowicz, P., Galerra, P., Pujol, J.P., 1999. Stimulating effect of diacerein on TGF-beta1 and beta2 expression in articular chondrocytes cultured with and without interleukin-1. *Osteoarthritis. Cartil. OARS, Osteoarthritis. Res. Soc.* 7, 255–264.
- Fernandes, L., Hagen, K.B., Bijlsma, J.W., Andreassen, O., Christensen, P., Conaghan, P.G., Doherty, M., Geenen, R., Hammond, A., Kjekken, I., Lohmander, L.S., Lund, H., Mallen, C.D., Nava, T., Oliver, S., Pavelka, K., Pitsillidou, I., da Silva, J.A., de la Torre, J., Zanoli, G., Vliet Ailand, T.P., 2013. EULAR recommendations for the non-pharmacological core management of hip and knee osteoarthritis. *Ann. Rheum. Dis.* 72, 1125–1135.
- Fernandez-Carballido, A., Herrero-Vanrell, R., Molina-Martinez, I.T., Pastoriza, P., 2004. Biodegradable ibuprofen-loaded PLGA microspheres for intraarticular administration. Effect of Labrafil addition on release in vitro. *Int. J. Pharm.* 279, 33–41.
- Fidelix, T.S., Macedo, C.R., Maxwell, L.J., Fernandes Moca Trevisani, V., 2014. Diacerein for osteoarthritis. *Cochrane Database Syst. Rev.* 2, CD005117.
- Gaignaux, A., Reeff, J., Siepmann, F., Siepmann, J., De Vriese, C., Goole, J., Amighi, K., 2012. Development and evaluation of sustained-release clonidine-loaded PLGA microparticles. *Int. J. Pharm.* 437, 20–28.
- Gao, Y., Chen, X., Fang, L., Liu, F., Cai, R., Peng, C., Qi, Y., 2014a. Rhein exerts pro- and anti-inflammatory actions by targeting IKKbeta inhibition in LPS-activated macrophages. *Free Radic. Biol. Med.* 72, 104–112.
- Gao, Y., Fang, L., Cai, R., Zong, C., Chen, X., Lu, J., Qi, Y., 2014b. Shuang-Huang-Lian exerts anti-inflammatory and anti-oxidative activities in lipopolysaccharide-stimulated murine alveolar macrophages. *Phytomedicine* 21, 461–469.
- Greten, F.R., Arkan, M.C., Bollrath, J., Hsu, L.-C., Goode, J., Miething, C., Göktuna, S.I., Neuenhahn, M., Fierer, J., Paxian, S., Van Rooijen, N., Xu, Y., O’Cain, T., Jaffee, B.B., Busch, D.H., Duyster, J., Schmid, R.M., Eckmann, L., Karin, M., 2008. NF- κ B is a negative regulator of IL-1 β secretion as revealed by genetic and pharmacological inhibition of IKK β . *Cell* 130, 918–931.
- Heo, S.-K., Yun, H.-J., Noh, E.-K., Park, S.-D., 2010. Emodin and rhein inhibit LIGHT-induced monocytes migration by blocking of ROS production. *Vasc. Pharmacol.* 53, 28–37.
- Hochberg, M.C., Altman, R.D., April, K.T., Benkhalti, M., Guyatt, G., McGowan, J., Towheed, T., Welch, V., Wells, G., Tugwell, P., 2012. American College of Rheumatology 2012 recommendations for the use of nonpharmacologic and pharmacologic therapies in osteoarthritis of the hand, hip, and knee. *Arthritis Care Res.* 64, 465–474.
- Horisawa, E., Kubota, K., Tuboi, I., Sato, K., Yamamoto, H., Takeuchi, H., Kawashima, Y., 2002. Size-dependency of DL-lactide/glycolide copolymer particulates for intra-articular delivery system on phagocytosis in rat synovium. *Pharm. Res.* 19, 132–139.
- Howie, D.W., Manthey, B., Hay, S., Vernon-Roberts, B., 1993. The synovial response to intraarticular injection in rats of polyethylene wear particles. *Clin. Orthop. Relat. Res.* 352–357.
- Kapoor, M., Martel-Pelletier, J., Lajeunesse, D., Pelletier, J.P., Fahmi, H., 2011. Role of proinflammatory cytokines in the pathophysiology of osteoarthritis. *Nat. Rev. Rheumatol.* 7, 33–42.
- Lee, S.C., Oh, J.T., Jang, M.H., Chung, S.I., 1999. Quantitative analysis of polyvinyl alcohol on the surface of poly(D,L-lactide-co-glycolide) microparticles prepared by solvent evaporation method: effect of particle size and PVA concentration. *J. Control. Release* 59, 123–132.
- Lee, J.-H., Koo, T.H., Yoon, H., Jung, H.S., Jin, H.Z., Lee, K., Hong, Y.-S., Lee, J.J., 2006. Inhibition of NF- κ B activation through targeting I κ B kinase by celastrol, a quinone methide triterpenoid. *Biochem. Pharmacol.* 72, 1311–1321.
- Legendre, F., Bogdanowicz, P., Martin, G., Domagala, F., Leclercq, S., Pujol, J.P., Ficheux, H., 2007. Rhein, a diacerein-derived metabolite, modulates the expression of matrix degrading enzymes and the cell proliferation of articular chondrocytes by inhibiting ERK and JNK-AP-1 dependent pathways. *Clin. Exp. Rheumatol.* 25, 546–555.
- Li, H., Guo, H., Wu, L., Zhang, Y., Chen, J., Liu, X., Cai, H., Zhang, K., Cai, B., 2013. Comparative pharmacokinetics study of three anthraquinones in rat plasma after oral administration of radix et rhei rhizoma extract and Dahuang Fuzi Tang by high performance liquid chromatography-mass spectrometry. *J. Pharm. Biomed. Anal.* 76, 215–218.
- Lorenz, H., Richter, W., 2006. Osteoarthritis: cellular and molecular changes in degenerating cartilage. *Prog. Histochem. Cytochem.* 40, 135–163.
- Louthrenou, W., Nilganuwong, S., Aksaranugraha, S., Asavatanabodee, P., Saengnipanthkul, S., the Thai Study, G., 2007. The efficacy, safety and carry-over effect of diacerein in the treatment of painful knee osteoarthritis: a randomised, double-blind, NSAID-controlled study. *Osteoarthritis. Cartil.* 15, 605–614.
- Mahajan, A., Singh, K., Tandon*, V.R., Kumar, S., Kumar, H., 2006. Diacerein: a new symptomatic slow acting drug for osteoarthritis. *J. Med. Educ. Res.* 8.
- Malaguti, C., Villela, C.A., Vieira, K.P., Souza, G.H., Hyslop, S., Zollner Rde, L., 2008. Diacerein downregulate proinflammatory cytokines expression and decrease the autoimmune diabetes frequency in nonobese diabetic (NOD) mice. *Int. Immunopharmacol.* 8, 782–791.
- Marinho, H.S., Real, C., Cyrne, L., Soares, H., Antunes, F., 2014. Hydrogen peroxide sensing, signaling and regulation of transcription factors. *Redox Biol.* 2, 535–562.
- Martel-Pelletier, J., Pelletier, J.P., 2010. Effects of diacerein at the molecular level in the osteoarthritis disease process. *Ther. Adv. Musculoskelet. Dis.* 2, 95–104.
- Martel-Pelletier, J., Mineau, F., Jolicoeur, F.C., Cloutier, J.M., Pelletier, J.P., 1998. In vitro effects of diacerein and rhein on interleukin 1 and tumor necrosis factor-alpha systems in human osteoarthritic synovium and chondrocytes. *J. Rheumatol.* 25, 753–762.
- Meissner, F., Molawi, K., Zychlinsky, A., 2008. Superoxide dismutase 1 regulates caspase-1 and endotoxic shock. *Nat. Immunol.* 9, 866–872.
- Moldovan, F., Pelletier, J., Jolicoeur, F.C., Cloutier, J.M., Martel-Pelletier, J., 2000. Diacerein and rhein reduce the ICE-induced IL-1 β and IL-18 activation in human osteoarthritic cartilage. *Osteoarthritis. Cartil.* 8, 186–196.
- Nicolas, P., Tod, M., Padoin, C., Petitjean, O., 1998. Clinical pharmacokinetics of diacerein. *Clin. Pharmacokinet.* 35, 347–359.
- Perruy, M., Guede, D., Lopez-Pena, M., Munoz, F., Caeiro, J.R., Gonzalez-Cantalapiedra, A., 2015. Effects of diacerein on cartilage and subchondral bone in early stages of osteoarthritis in a rabbit model. *BMC Vet. Res.* 11, 143.
- Qvist, P., Bay-Jensen, A.C., Christiansen, C., Dam, E.B., Pastoureau, P., Karsdal, M.A., 2008. The disease modifying osteoarthritis drug (DMOAD): is it in the horizon? *Pharmacol. Res.* 58, 1–7.
- Ratcliffe, J.H., Hunneyball, I.M., Smith, A., Wilson, C.G., Davis, S.S., 1984. Preparation and evaluation of biodegradable polymeric systems for the intra-articular delivery of drugs. *J. Pharm. Pharmacol.* 36, 431–436.
- Ratcliffe, J.H., Hunneyball, I.M., Wilson, C.G., Smith, A., Davis, S.S., 1987. Albumin microspheres for intra-articular drug delivery: investigation of their retention in normal and arthritic knee joints of rabbits. *J. Pharm. Pharmacol.* 39, 290–295.
- Roy, K., Kanwar, R.K., Kanwar, J.R., 2015. Molecular targets in arthritis and recent trends in nanotherapy. *Int. J. Nanomedicine* 10, 5407–5420.
- Salazar, J., Bello, L., Chavez, M., Anez, R., Rojas, J., Bermudez, V., 2014. Glucosamine for osteoarthritis: biological effects, clinical efficacy, and safety on glucose metabolism. *Arthritis* 2014, 432463.
- Sauerschnig, M., Stolberg-Stolberg, J., Schulze, A., Salzmann, G.M., Perka, C., Dinybil, C.J., 2014. Diverse expression of selected cytokines and proteinases in synovial fluid obtained from osteoarthritic and healthy human knee joints. *Eur. J. Med. Res.* 19, 65.
- Shive, M.S., Anderson, J.M., 1997. Biodegradation and biocompatibility of PLA and PLGA microspheres. *Adv. Drug Deliv. Rev.* 28, 5–24.
- Siepmann, J., Faisant, N., Benoit, J.P., 2002. A new mathematical model quantifying drug release from bioerodible microparticles using Monte Carlo simulations. *Pharm. Res.* 19, 1885–1893.
- Sokolove, J., Lepus, C.M., 2013. Role of inflammation in the pathogenesis of osteoarthritis: latest findings and interpretations. *Ther. Adv. Musculoskelet. Dis.* 5, 77–94.
- Stevenson, C.L., Santini Jr., J.T., Langer, R., 2012. Reservoir-based drug delivery systems utilizing microtechnology. *Adv. Drug Deliv. Rev.* 64, 1590–1602.
- Sun, H., Yin, Q., Zhang, A., Wang, X., 2012. UPLC-MS/MS performing pharmacokinetic and biodistribution studies of rhein. *J. Sep. Sci.* 35, 2063–2068.
- Tak, P.P., Firestein, G.S., 2011. NF-kappaB: a key role in inflammatory diseases. *J. Clin. Invest.* 107, 7–11.
- Tamura, T., Kosaka, N., Ishiwa, J., Sato, T., Nagase, H., Ito, A., 2001. Rhein, an active metabolite of diacerein, down-regulates the production of pro-matrix metalloproteinases-1, -3, -9 and -13 and up-regulates the production of tissue inhibitor of metalloproteinase-1 in cultured rabbit articular chondrocytes. *Osteoarthritis. Cartil.* 9, 257–263.
- Tamura, T., Shirai, T., Kosaka, N., Ohmori, K., Takafumi, N., 2002. Pharmacological studies of diacerein in animal models of inflammation, arthritis and bone resorption. *Eur. J. Pharmacol.* 448, 81–87.
- Toegel, S., Wu, S.Q., Piana, C., Unger, F.M., Wirth, M., Goldring, M.B., Gabor, F., Viernstein, H., 2008. Comparison between chondroprotective effects of glucosamine, curcumin, and diacerein in IL-1 β -stimulated C-2812 chondrocytes. *Osteoarthritis. Cartil.* 16, 1205–1212.
- Verbruggen, G., 2006. Chondroprotective drugs in degenerative joint diseases. *Rheumatology (Oxford, England)* 45, 129–138.
- Wojdasiewicz, P., Poniatowski, L.A., Szukiewicz, D., 2014. The role of inflammatory and anti-inflammatory cytokines in the pathogenesis of osteoarthritis. *Mediat. Inflamm.* 2014, 561459.
- Yang, R., Yang, L., Shen, X., Cheng, W., Zhao, B., Ali, K.H., Qian, Z., Ji, H., 2012. Suppression of NF-kappaB pathway by crocetin contributes to attenuation of lipopolysaccharide-induced acute lung injury in mice. *Eur. J. Pharmacol.* 674, 391–396.
- Yang, L., Zhang, J., Wang, G., 2015. The effect of sodium hyaluronate treating knee osteoarthritis on synovial fluid interleukin-1 beta and clinical treatment mechanism. *Pak. J. Pharm. Sci.* 28, 407–410.
- Yaron, M., Shirazi, I., Yaron, I., 1999. Anti-interleukin-1 effects of diacerein and rhein in human osteoarthritic synovial tissue and cartilage cultures. *Osteoarthritis. Cartil. OARS, Osteoarthritis. Res. Soc.* 7, 272–280.
- Zhang, W., Nuki, G., Moskowitz, R.W., Abramson, S., Altman, R.D., Arden, N.K., Bierma-Zeinstra, S., Brandt, K.D., Croft, P., Doherty, M., Dougados, M., Hochberg, M., Hunter, D.J., Kwoh, K., Lohmander, L.S., Tugwell, P., 2010. OARSI recommendations for the management of hip and knee osteoarthritis: part III: changes in evidence following systematic cumulative update of research published through January 2009. *Osteoarthritis. Cartil. OARS, Osteoarthritis. Res. Soc.* 18, 476–499.